High power tunable diode-pumped Yb3+:CaF2 laser

A. Lucca, Mathieu Jacquemet, Frédéric Druon, François Balembois, Patrick
Georges, Patrice Camy, Jean-Louis Doualan, Richard Moncorgé

High-power tunable diode-pumped Yb³⁺:CaF₂ laser

A. Lucca, M. Jacquemet, F. Druon, F. Balembois, and P. Georges

Laboratoire Charles Fabry de l'Institut d'Optique, du Centre National de la Recherche Scientifique et de l'Université Paris-Sud Centre Universitaire, Batiment 503, 91403 Orsay Cedex, France

P. Camy, J. L. Doualan, and R. Moncorgé

Centre Interdisciplinaire de Recherche Ions Lasers, Unite Mixte de Recherche 6637, Centre National de la Recherche Scientifique, Commissariat à l'Energie Atomique, Institut des Sciences de la Matiére et du Rayonnement, Université de Caen, 6 Boulevard du Maréchal Juin, 14050 Caen Cedex 4, France

Results of diode-pumped cw laser operation of an Yb³⁺:CaF₂ single crystal are reported for what is to our knowledge the first time. With a 5-at.% Yb³⁺-doped sample we obtained 5.8-W output power at 1053 nm for 15 W of incident power at 980 nm. The laser wavelength could be tuned from 1018 to 1072 nm, and a small-signal gain as high as 1.8 was achieved, showing the great potential of Yb³⁺:CaF₂ as an amplifier medium for femtosecond pulses.   © 2004 Optical Society of America

OCIS codes: 140.3380, 140.3480, 140.5680, 140.3070.

Interest in Yb³⁺-doped materials is still growing, owing to the increasing availability of high-power, high-brightness InGaAs laser diodes emitting near 980 nm. For numerous applications near 1.05 μm, Yb³⁺-doped materials exhibit various advantages compared with their Nd³⁺ counterparts. The fact that there are only two electronic multiplets in the near-infrared spectral domain[1] leads to very low quantum defects (typically <10%), reducing thermal loads and preventing undesired effects such as upconversion and excited-state absorption. The absence of these effects permits high dopant concentrations while maintaining low fluorescence quenching and gives rise to high efficiencies even at high pump powers.[2] The longer emission lifetimes of Yb³⁺-doped materials ensure higher energy-storage capabilities. Finally, because of stronger electron–phonon interaction, the broader absorption and emission spectra of these materials allow diode pumping with relaxed temperature regulation constraints, wide tunabilities, and the production of ultrashort pulses.[3] For scaling the power that is achievable from Yb³⁺-based crystals, which will permit exploitation of these favorable characteristics, hosts with high thermal conductivities are desirable. In this context we decided to grow, study, and operate various CaF₂ single crystals with different Yb-doping levels.

CaF₂ is a well-known crystal that can be grown rather easily both in the form of large, good-quality bulk crystals by use of the Bridgman or the Czochralski technique and in the form of thin films by use of molecular beam epitaxy or liquid phase epitaxy. Because of its exceptional transparency (0.15−9 μm), CaF₂ is commonly used to build commercial optics and devices in the ultraviolet as well as in the infrared spectral domain. It is now more particularly studied for use in submicrometer photolithography and can be produced in large size and quantity. The optical properties of fluoride structures such as CaF₂ doped by trivalent rare-earth ions have been investigated for years[4]: the substitution of Yb³⁺ for Ca²⁺ ions and the resulting necessary charge compensation typically give rise to a rich multisite structure that leads to broad absorption and emission bands, comparable to those of glasses,[5] which is important, as mentioned above, for diode pumping as well as for the production of broadly tunable femtosecond laser sources. The cubic structure of this crystal implies the independence of absorption from pump polarization and the absence of any favorite polarization for the emitted light. Although CaF₂ material can already be produced with large dimensions as single crystals, its cubic structure also makes CaF₂ potentially suitable as a ceramic laser host,[6] opening the way to all the advantages in laser design that are supplied by this technology.[7] Moreover, the thermal conductivity of this crystal, at least when it is undoped, is 9.7 W m⁻¹ K⁻¹, similar to that found for YAG and nearly twice that of other low-phonon fluoride crystals, such as LiCaAlF₆ or LiYF₄.[8] Even if CaF₂ exhibits a lower thermal conductivity when it is doped with rare-earth ions (we estimated the conductivity at ∼4 W m⁻¹ K⁻¹ for a 5-at.% doping level, using the method presented in Ref. 9), the spectroscopic and laser properties of Yb³⁺:CaF₂ are worth examining, which was not done until recently.[10,11] The availability of proper laser diode sources for direct pumping thus persuaded us to undertake a detailed analysis of its optical properties and to investigate its laser potentiality under high-pump-power conditions.

Spectroscopic and laser crystals were grown by use of the Bridgman technique in an Ar and CF₄ atmosphere to eliminate parasitic traces of oxygen ions. At low temperature (7 K), with a low doping level of ∼0.115-at.% Yb, the absorption and emission spectra are well structured and exhibit the typical three different kinds of trivalent rare-earth ion sites that are usually found in CaF₂.[4] At room temperature and with greater than ∼0.5-at.% Yb, as expected and as shown in Fig. 1, the absorption and emission bands are broad and weakly structured, comparable to those found, for example, in the case of Yb:QX phosphate glass.[3,5] Figure 1 shows, for Yb:CaF₂, room-temperature gain cross sections σ_g, obtained for
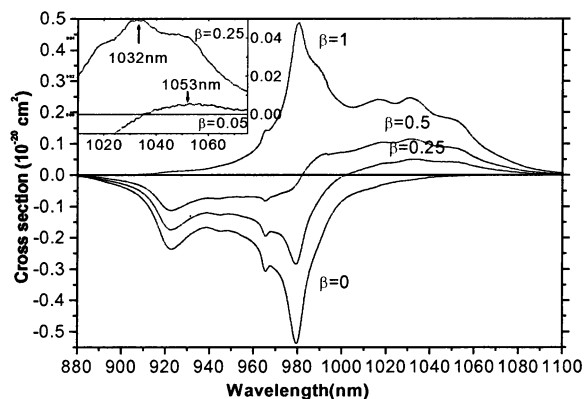
Fig. 1. Gain cross section (σ_g) of Yb:CaF$_2$ for different values of population inversion rate $\beta = N_2/N$. $\sigma_g = \beta\sigma_e - (1 - \beta)\sigma_a$. σ_e and σ_a are emission and absorption cross sections, respectively. For $\beta = 0$ we obtain the absorption cross section; for $\beta = 1$ we obtain the emission cross section.

different values of excited-state population fraction β ($\beta = N_2/N$). The gain cross section is defined as $\sigma_g = \beta\sigma_e - (1 - \beta)\sigma_a$, and the absorption and emission cross-section curves, σ_a and σ_e, respectively, are given for the values $\beta = 0$ and $\beta = 1$, respectively.

Absorption and emission cross-section peaks are located near 980 nm, with a value of $\sim 0.55 \times 10^{-20}$ cm^2. It is worth noting that there is an absorption peak near 923 nm, which could be useful for optical pumping when lasing occurs at shorter wavelengths, ~ 1 μm. We also note that the emission spectrum extends up to nearly 1080 nm, which is promising for the development of new broadly tunable laser sources, as well as for the design of femtosecond oscillators or amplifiers. Independently of the samples (powders or bulky crystals) and of the doping level, the lifetime of the metastable level $^2F_{5/2}$ is 2.4 ms, which is relatively long for an Yb^{3+}-doped material, being 0.35 ms for the KY(WO$_4$),[12] 1.3 ms for the QX glass, 1.1 ms for the Sr^{3}Y(BO^3)^3 (BOYS), 0.95 ms for the YAG,[5] 2.4 ms for the Ca^{4}GdO(BO^3)^3 (YCOB),[13] 2.44 ms for the GdCOB,[14] and 2 ms for the YLF.[15] These results are encouraging in terms of energy storage and laser power capability.

The laser setup is shown in Fig. 2. The pump source was a fiber-coupled laser diode emitting up to 15 W near 980 nm, with a 200-μm fiber core diameter and a numerical aperture of 0.22, supplied by LIMO. The selected crystal was an uncoated 5-at. % Yb^{3+}-doped sample that was 4 mm long, with parallel, polished end faces. The pump beam was focused into the active medium by two 60-mm focal-length doublets. The resonator was a stable three-mirror folded cavity designed to support only TEM$_{00}$ oscillation and to focus the mode to a beam radius of nearly 100 μm inside the crystal. We adjusted the diode temperature to force the pump wavelength to match the Yb^{3+}:CaF$_2$ absorption peak at maximum pump power, allowing the crystal to absorb up to nearly 11 W (approximately 70% of the total incident power). We avoided thermal fracture by use of indium foils to connect the crystal to a water-cooled copper mount.

The results of the Yb^{3+}:CaF$_2$ laser action are plotted in Fig. 3: a laser output power of 5.8 W at 1053 nm, a threshold pump power of 2 W, and a laser slope efficiency of nearly 45% with respect to incident pump power were obtained by use of a 6% transmission output coupler. This is, to our knowledge, the first demonstration of diode-pumped laser operation ever obtained with Yb^{3+}:CaF$_2$. The laser kept working TEM$_{00}$ at any level of incident pump power, and the output beam did not exhibit any favorite polarization.

Other Yb^{3+}:CaF$_2$ laser samples with higher doping levels were also tested. Using a 2.5-mm-long, uncoated, 8.9-at. % Yb^{3+}-doped crystal, we obtained 1.5-W output power for 13-W incident power. At that pumping level, at which 10 W was absorbed, the sample rapidly suffered (after a few minutes) from thermal fractures. Another 2-mm-long, 12-at. % Yb^{3+}-doped crystal, pumped by 15-W incident power, absorbed up to 9 W but exhibited thermal fractures almost instantaneously, preventing us from testing its laser properties.

Wavelength tuning was achieved by insertion of an SF10 dispersive prism inside the collimated arm of the cavity. The results are presented in Fig. 4. The crystal provided laser action over a continuous range broader than 54 nm, from 1017.8 to 1072.1 nm, with a maximum near 1052 nm. Prism insertion increased
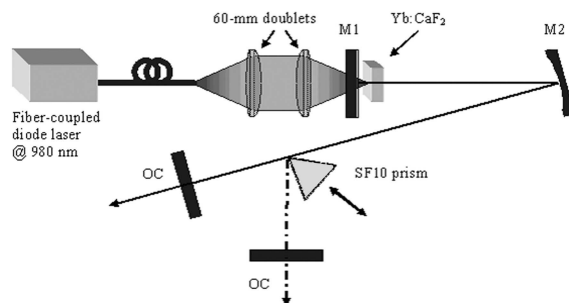

Fig. 2. Experimental setup: M1, flat dichroic mirror (highly reflective at 1020–1200 nm and highly transmissive at 980 nm); M2, concave mirror (radius of curvature 200 mm, highly reflective at 1020–1200 nm); OCs, output couplers. Arm lengths: M1–M2 $\sim$ 120 mm, M2–OC $\sim$ 300 mm.
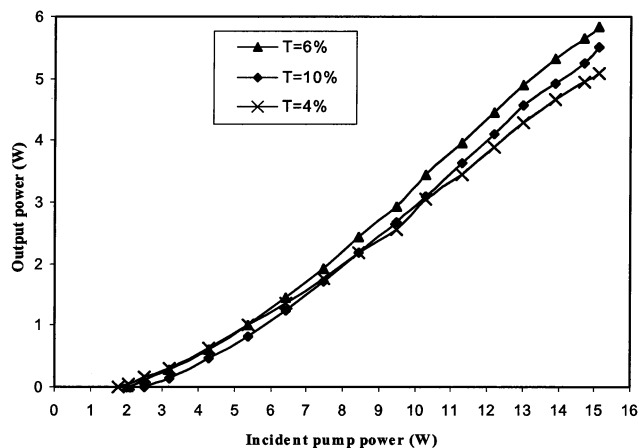

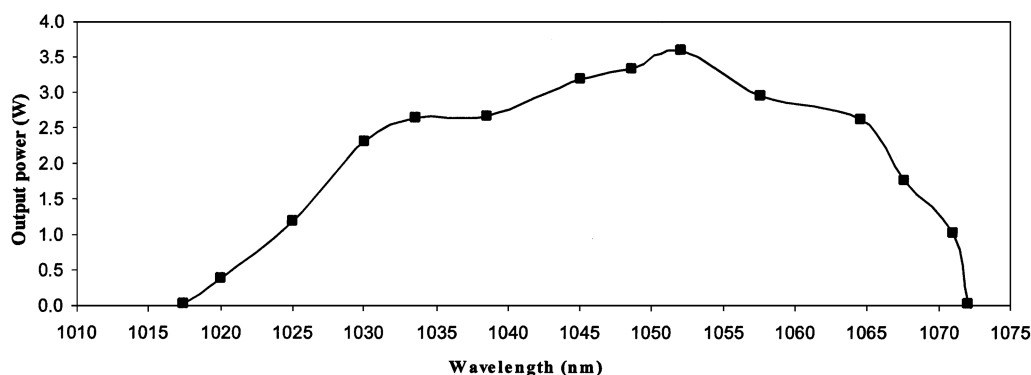Fig. 3. Output power versus incident power for different output couplers.

Fig. 4.   Tuning curve of Yb:CaF$_2$ with an SF10 dispersive prism and a 6% transmission output coupler.

intracavity losses, forcing horizontal polarization and causing a 35% decrease of output power. Short-wavelength laser operation is limited by a dichroic mirror's coatings. In fact, Yb:CaF$_2$ laser action down to 1000 nm was recently demonstrated with a Ti:sapphire laser at 923 nm as the pump source.[11]   We expect to reach even lower wavelengths soon under diode pumping near 920 nm by employing appropriate mirrors and other cavity schemes, such as off-axis pumping.[16]

Preserving the configuration of our oscillator, we finally replaced the output coupler, increasing its transmission, to estimate small-signal gain in our crystal. Laser action was achieved with a 45% transmission output coupler and with 13-W incident pump power. An output power of 500 mW was thus obtained at 1032 nm. Losses increased as the output mirror transmission increased, thus forcing the laser to oscillate at a shorter wavelength, as shown in Fig. 1, in which the gain cross section is larger than it is at 1053 nm. We estimate a double-pass gain of more than ~1.8. Even if other Yb hosts exhibit a higher gain cross section,[1,14] this gain of 1.8 confirms that Yb:CaF$_2$ could be suitable for the development of large laser modes femtosecond oscillators as well as amplifiers.[17]

In conclusion, we have presented the first diode-pumped laser based on Yb:CaF$_2$ crystal. Up to 5.8 W of laser output power was produced near 1053 nm, and the laser wavelength could be tuned over more than 54 nm. A double-pass small-signal gain higher than 1.8 was measured. Yb:CaF$_2$ crystals exhibit interesting properties in terms of thermal conductivity, tunability, efficiency, and gain, and they can be grown rather easily by standard techniques, resulting in large size and excellent optical quality. These reasons and our results allow us to suppose that, in the near future, Yb:CaF$_2$ could represent one of the best choices in the field of solid-state lasers for high-power diode-pumped broadly tunable cw sources as well as for femtosecond pulse generation or amplification.

References

1. L. D. De Loach, S. A. Payne, L. L. Chase, L. K. Smith, W. L. Kway, and W. F. Krupke, IEEE J. Quantum Electron. **29,** 1179 (1993).
2. D. S. Sumida, A. A. Betin, H. Bruesselbach, R. Bryen, S. Matthews, R. Reeder, and M. S. Mangir, Laser Focus World **35**(6), 6370 (1999).
3. C. Hönninger, R. Paschotta, M. Graf, F. Morier-Genoud, G. Zhang, M. Moser, S. Biswal, J. Nees, A. Braun, G. A. Mourou, I. Johannsen, A. Giesen, W. Seeber, and U. Keller, Appl. Phys. B **69,** 3 (1999).
4. W. Hayes, *Crystals with the Fluorite Structure* (Clarendon, Oxford, England, 1974).
5. S. Chenais, F. Druon, F. Balembois, P. Georges, R. Gaume, P. H. Haumesser, B. Viana, G. P. Aka, and D. Vivien, J. Opt. Soc. Am. B **19,** 1083 (2002).
6. S. E. Hatch, W. F. Parsons, and R. J. Weagley, Appl. Phys. Lett. **5,** 153 (1964).
7. J. Lu, J. F. Bisson, K. Takaichi, T. Uematsu, A. Shirakawa, M. Musha, K. Ueda, H. Yagi, T. Yanagitani, and A. A. Kaminskii, Appl. Phys. Lett. **83,** 1101 (2003).
8. J. L. Doualan and R. Moncorge, Ann. Chim. Sci. Mat. **28,** 5 (2003).
9. R. Gaume and B. Viana, Ann. Chim. Sci. Mat. **28,** 89 (2003).
10. M. Ito, C. Goutaudier, Y. Guyot, K. Lebbou, T. Fukuda, and G. Boulon, J. Phys. Condens. Matter **16,** 1501 (2004).
11. V. Petit, J. L. Doualan, P. Camy, V. Mesnard, and R. Moncorgé, Appl. Phys. B **78,** 681 (2004).
12. A. A. Demidovich, A. N. Kuzmin, G. I. Ryabtsev, M. B. Danailov, W. Strek, and A. N. Titov, J. Alloys Compd. **300,** 238 (2000).
13. A. Aron, G. Aka, B. Viana, A. Kahn-Harari, D. Vivien, F. Druon, F. Balembois, P. Georges, A. Brun, N. Lenain, and M. Jacquet, Opt. Mater. **16,** 181 (2001).
14. S. Chénais, F. Druon, F. Balembois, G. Lucas-Leclin, P. Georges, A. Brun, M. Zavelani-Rossi, F. Augé, J. P. Chambaret, G. Aka, and D. Vivien, Appl. Phys. B **72,** 389 (2001).
15. N. Uehara, K. Ueda, and Y. Kubota, Jpn. J. Appl. Phys. **35,** L499 (1996).
16. M. Jacquemet, F. Balembois, S. Chénais, F. Druon, P. Georges, R. Gaumé, and B. Ferrand, Appl. Phys. B **78,** 13 (2004).
17. P. Raybaut, F. Druon, F. Balembois, P. Georges, R. Gaumé, B. Viana, and D. Vivien, Opt. Lett. **28,** 2195 (2003).